Protein dynamics without energy landscape: a rotation-translation model combining elastic, time domain and multiple neutron scattering.

Wolfgang Doster[1] and Marie-Sousai Appavou[2]

[1]Technical University Munich, Physics Department E 13 and FRM 2, D-85748 Garching, Germany

[2]Jülich Centre for Neutron Science, Forschungszentrum Jülich GmbH, Outstation at MLZ, Lichtenbergstraße 1, D-85747 Garching, Germany

Abstract

We address the question, whether proteins as 'complex systems' can be characterized dynamically by specific spatial motions, instead of resorting to heterogeneous diffusion in energy space. The neutron scattering spectra of dry and hydrated myoglobin are analyzed in the time domain based on a generic dynamic model with two major components, rotational transitions of side chains, mainly methyl groups and local translational diffusion of non-methyl side chains. The significance of the fits is based on data covering a wide range in time, momentum exchange and temperature. The spectra of three spectrometers with overlapping energy range are Fourier transformed to the time domain from 10^{-13} to 10^{-9} s. In the hydrated case, regular exponential methyl group reorientation is observed on a 10 picosecond time scale. In the dehydrated system this process is slowed down by a factor of two and a further dispersion to even slower correlation times occurs. The local diffusion of non-methyl side chains varies strongly with the water content. It is absent in the dehydrated system. At full hydration, the respective correlation times ~ 150 ps overlap with those observed for hydration water, suggesting a close coupling. The translation-rotation model applies the established theory of space time correlation functions successfully, which is compatible with the idea of homogeneous quasi-elastic spectra. The temperature dependent elastic intensity extrapolated to zero momentum exchange is derived from the unavoidable effects of multiple scattering, independent of energy landscapes.

I. Introduction

Neutron scattering is a technique to record the time resolved displacement distribution of mainly hydrogen atoms in bio-molecules. From the self-interference of neutrons scattered locally by individual nuclei according to their cross-section, specially designed spectrometers derive space-time correlation functions of local molecular displacements. The well-established spatial scattering theory has been challenged recently by Frauenfelder et al.[1,2], suggesting that neutrons interact instead globally with the protein performing an energy controlled random walk in conformational space. We show that some of the claimed heterogeneity effects are due to multiple scattering. Second, a two component dynamic model of rotational and translational motions using space-time correlation functions is shown to predict the outcome of neutron scattering experiments accurately.

Most published experiments up to date focus on elastic scattering. In the preceding paper we have shown, how to derive dynamic information from elastic spectra[3]. In this work we expand the frame to include inelastic spectra. The first dynamic neutron scattering experiments at subzero temperatures were performed in 1989 with dry and hydrated myoglobin[4-7]. Two specific molecular processes could be distinguished by their temperature dependence using thermally stable D_2O- hydrated powders instead of solutions[4]. In hydrated samples, global protein diffusion is arrested, emphasizing the spectral contribution of internal structural fluctuations. Elastic scans versus the temperature revealed two dynamical transitions by the abrupt increase of hydrogen displacements above 150 K and 240 K[5,8]. By fitting an analytical model to the observed elastic scattering function, the processes were assigned to two-(or three) state transitions of side chains (type R) and water-coupled diffusion of residues on a small scale (type T)[5,8]. The type T transition, characterized as a cross-over of

relaxation time and instrumental resolution from the inelastic spectrum, was denoted as a 'dynamical transition' because of its connection with the glass transition of hydration water[5]. The low temperature transition at 150-180 K was incorrectly characterized as a de-trapping of torsional transitions controlled by the glass transition of hydration water. Today, type T is still assigned to water coupled local diffusion, while type R was shown to reflect mostly rotational transitions of the methyl groups[3,8,26-29]. In the original model the two processes were convoluted sequentially, implying identical scattering sites, performing two kinds of motion. We employ high quality spectra, combining data of three neutron spectrometers, which are transformed to the time domain. From this new data base we derive a model of minimal complexity, comprising the original two types of molecular motions in a parallel manner[5,8] .

Neutron scattering emphasizes the hydrogens, which constitute nearly half of the atoms in proteins. They mediate H-bridges in helices and take part in other nonbonding interactions of electrostatic and van der Waals forces. Polar bonds play a critical role in enzyme catalysis, substrate binding and proton transfer reactions. Main chain and side chain hydrogens contribute to the stability of the protein secondary structure and mediate structural fluctuations. Neutron diffraction yields precise hydrogen positions and fluctuation amplitudes in excess to x-ray crystallography, since the hydrogen cross section is comparable to the carbon[9,10]. A particularly useful property of the proton is its large incoherent cross section, about ten times larger than those of other atoms. As a result, 85 % of the scattering amplitude of proteins reflects hydrogen atoms[10]. The scattering contribution of hydration water in D_2O-hydrated powders can be kept as low as 4 % [10]. Energy resolved spectra, Fourier-transformed to the time domain, yield a hydrogen weighted density correlation function of structural

fluctuations. The basic physical quantity of interest is the density self-correlation function $G_s(\vec{r}, t)$ characterizing the distribution of single particle displacements $\vec{r}$ within time t. For isotropic powder samples only the magnitude of $\vec{r}$ matters. In scattering experiments one measures the intermediate scattering function in momentum-space, which is the Fourier transform of the density correlation function[11-13]:

$$\Phi_s(Q,t) = < \int d^3\vec{r} \cdot e^{-i\vec{Q}\cdot\vec{r}} G_s(\vec{r},t) >_{powder} \quad (1)$$

The resulting powder averaged intermediate scattering function $\Phi_s(Q, t)$ of N hydrogen atoms can be expanded in terms of Q^2 as follows [8,13]:

$$\Phi_s(Q,t) = \frac{1}{N}\sum_i \Phi_i(Q,t)) = \frac{1}{N}\sum_i \exp\left[-Q^2\left\langle \Delta x_i^2(t)\right\rangle/2 + Q^4 .....\right] \quad (2)$$

Q denotes the magnitude of the scattering vector, $Q = (4\pi/\lambda)\cdot\sin(\theta/2)$, λ is the incoming neutron wavelength and θ is the scattering angle relative to the incident direction. Equ.(2) is known as the Placzek moment expansion of the powder averaged hydrogen displacement distribution $G_s(r, t)$. The second moment, $<\Delta x_i^2(t)>$, defines the x-mean square displacement (MSD) of a specific site 'i' at time t. At low Q, $\Phi_s(Q\rightarrow 0, t)$, the "Gaussian" approximation yields the site averaged MSD: $<\Delta x^2>_t = \Sigma<\Delta x_i^2>/N$.

Most bio-neutron scattering studies up to date deal with elastic scattering experiments[3]. Temperature dependent MSD scans were measured for numerous proteins under different environmental conditions. Fig. 1 summarizes some essential results for myoglobin derived from elastic profiles similar to those presented in fig. 5a:[5,8]: Vibrational displacements are characterized by a linear MSD temperature dependence. This applies to myoglobin embedded in a D-exchanged hydrogenated sucrose glass, suggesting that vitrified proteins do not move[14,15]. By contrast, with

myoglobin embedded in a fully deuterated glass, D-glucose, a strong nonlinear enhancement of $<\Delta x^2>(T)$ at 150 K appears[8]. Strikingly, dehydrated myoglobin exhibits about the same MSD temperature dependence as myoglobin vitrified in a per-deuterated glass[8]. The transition at 150 K is thus denoted as type R, attributed to the onset of protein internal motions, which are not sensitive to changes of the protein environment. By contrast, with D_2O-hydrated myoglobin, two transition temperatures at 150 K (type R) and 240 K (type T) are recorded, suggesting two well separated molecular processes. Since the second transition (type T) does not occur without water, these motions were assigned to protein displacements related to a wet protein surface[5,8]. Since the scattering fraction of hydration water (D_2O) amounts to less than 5 %, type II motions characterize the indirect effect of hydration on structural fluctuations. Experiments, performed with "wet" per-deuterated purple membrane fragments, yield similar, but noisier MSD scans with two transition temperatures at 150 and 240 K[14,15]. By contrast, if the per-deuterated purple membrane fragments are specifically labelled with protonated, but methyl-free residues, the type R transition is missing, although type T at 240 K still occurs[9]. This result proves, that type R displacements reflect mostly methyl side chains[8,16]. Type T by contrast involves prominently polar residues near the surface. An indirect effect of hydration on the mobility of nonpolar, non-methyl side chains by swelling effects cannot be excluded. In solutions one has to account for global protein diffusion[17]. Only a single dynamical transition at ~200 K is observed with Mössbauer spectroscopy of myoglobin, recording the motions of the heme iron. It was assigned to type T dynamics, because it varies with the solvent viscosity[3,18].

The second moment reflects only behavior of the elastic scattering function at low Q. The complete elastic profile, $\sim \Phi(Q, t = \tau_{res})$, can be used as input to determine $G_s(r, t)$

by inverting equation (1) numerically. Unfortunately, the available Q-range is too small to render such a procedure successful. An analytical transform, expanding the elastic scans by a sum of Gaussian distributions is technically feasible. This was first demonstrated in ref.(8) with two Gaussians. Here this method is repeated with the improved data set of fig. 5a. Fig. 2 shows the reconstructed $G_s(r, t)$, which exhibits the shape of a bimodal displacement distribution as it evolves with the temperature. Up to 200 K a single, temperature independent maximum is observed, reflecting protein vibrations. Above 200 K, two peaks at r ≅ 0,5 Å and 1,5 Å emerge. The first maximum, reflecting small scale displacements, vibration and local diffusion, appears only with hydrated proteins as the red curve shows. It is connected with the onset of un-harmonic displacements above 240 K. This suggests the involvement of polar side chains near the protein surface of type T.

The second maximum (type R) occurs in hydrated, but also in dehydrated (red) and glassy protein environments. It accounts for the low temperature transition of the methyl group rotation at 150 K.

II. Methods

Previously published neutron scattering experiments with dry and hydrated, performed with the spectrometers IN6, IN10 and IN13 at the ILL in Grenoble, are reanalyzed[5-8,20]. Such a combination of high quality data obtained with the same sample is rare and difficult to obtain. The analysis relies heavily on inelastic back-scattering experiments at high Q, which, because of the low flux, requires several days of beam time for a single temperature. The frequency domain spectra are transformed to the time domain[19]. Taken together this new analysis covers a large Q^2-range up to 25 $Å^{-1}$, combined with a time window ranging from 0,1 to 1000 picoseconds. The recorded dynamical structure factor, $S(\theta, \hbar\omega)$, versus scattering

angle θ and energy exchange ħω, is transformed to a constant Q format, S(Q, ħω), which is then symmetrized by the detailed-balance factor. The time domain correlation function $\Phi_s(Q, t)$ is determined numerically by turning the Fourier integral of S(Q, ω) into a sum of discrete points using the experimental spectrum $S(Q, \omega_j)$:

$$\Phi_s(Q,t) = \hbar \int d\omega\, e^{i\omega \cdot t} S(Q,\omega) \cong \hbar \cdot \Delta\omega \cdot \sum_j e^{i\omega_j \cdot t} S(Q,\omega_j) \qquad (3)$$

To avoid aliasing effects the smooth spectra $S(Q, \omega_j)$ are interpolated with a maximum number of n data points according to $t_n = n \cdot \frac{\pi}{\omega_{max}}$ (FFT), where ω_{max} is the cut-off frequency of the spectrum. As a consistency check the transformed result is back-transformed to the frequency domain. To de-convolute the data from the resolution function, a time domain low temperature spectrum of Mb-D_2O at 100 K was determined. The elastic intensity was collected using a fixed energy window method (τ_{res} = 140 ps) and the back-scattering spectrometer IN13[11]. With 350 mg of D_2O hydrated horse heart-myoglobin (h = 0,35-0,38 g/g), the neutron transmission was close to a tolerable 90 %. Raw data were corrected for detector response and cell scattering.

III. Results

a) Definition of the translation-rotation model (TR)

Motivated by the results of fig. 1 and 2, we propose a bimodal distribution of sites associated with two kinds of motions: Internal rotational transitions (R) and local translational diffusive displacements (T). Thus a bimodal correlation function of two major components is assumed:

$$\Phi_s(Q,t) = \sigma_R \cdot \Phi_R(Q,t) + (1-\sigma_R) \cdot \Phi_T(Q,t) \qquad (4)$$

σ_R denotes the fractional cross section of the type R sites.

Equ. (4) must be complemented by a term accounting for global protein diffusion, if the degree of hydration exceeds 0,4 g/g as in solution[17].

According to the neutron structure of myoglobin 25 -28 % of the total number of hydrogens are organized in methyl groups, thus $\sigma_I = \sigma_m \cong 0{,}25$ -0,28[9].

More specifically, R-type motions are approximated by a three site jump model of groups reorienting by 120° jumps about their three-fold symmetry axis[11]:

$$\Phi_R(Q,t) = \frac{1}{3}\{1 + 2j_0(Q) + 2\cdot(1 - j_0(Q))\cdot\exp(-t/\tau_{rot})\} \qquad (5)$$

$$j_0(Q) = \sin(Q\sqrt{3}\cdot r)/(Q\sqrt{3}\cdot r)$$

is the zero order Bessel function, where r = 1,03 Å is the length of the C-H bond. Exponential relaxation or a single barrier height is assumed for simplicity. Note that $\tau_{rot} = \tau_{Met}/3$ and that the $EISF_{met}(Q) = \Phi(Q, t >> \tau_{rot})$ is not Gaussian.

By contrast, translational processes involve residues displacements confined by a quasi- harmonic potential. The most general approach to Brownian motion in a harmonic potential is the Ornstein-Uhlenbeck process, which reduces to a Smoluchovski equation in the over-damped case as will be discussed elsewhere.

The resulting powder averaged intermediate scattering function of local diffusion is given by [20,21,32]:

$$\Phi_T(Q,t) = \exp\{-Q^2\delta^2\cdot(1 - \exp(-t/\tau_{trans}))\} \qquad (6)$$

$\delta^2 = \langle\Delta x^2\rangle$ denotes the translational mean square displacement of local diffusion without vibrational displacements. τ_{trans} is the relaxation time of local diffusion. Thus only two parameters are required to adjust the translational component. At long times, $\Phi_T(Q, t >> \tau_{trans})$ turns into a Gaussian elastic scattering function:

$$\Phi_T(Q, t >> \tau_{trans}) = \exp(-Q^2\cdot\delta^2) \qquad (7)$$

The TR-model with two main components is defined by the equations 4 – 6.

b) Time domain analysis

Fig. 3 displays the combination of three transformed intermediate scattering functions of dry and D_2O hydrated myoglobin at 300 K. The initial decay at 0,1 picoseconds reflects the vibrational dephasing of the Boson peak, which differs for dry and hydrated myoglobin[4]. We analyze the over-damped regime above 1ps, where the correlation functions have been normalized. Vibrational displacements are thus not included.

In the hydrated case, the decay of the correlation function covers at least three decades, which is difficult to interpret without assistance of a theoretical model. The full line shows the prediction of the TR model at Q = 1,9 $Å^{-1}$ to be accurate. Alternative predictions at Q = 1 and 2,5 $Å^{-1}$ deviate strongly, illustrating the sensitivity of the model. The methyl group relaxation is well represented by an exponential decay (short dash), leading to a Q-dependent long-time plateau at 0,8. The Brownian oscillator correlation function is non-exponential. Its long time value is given by equ. 7. We derive two well separated components with time constants at τ_{rot} = 9 (±1) ps and τ_{trans} = 145 (±15) ps. This result confirms the analysis of figs. 1 and 2 displaying two well separated onset temperatures and displacement distribution maxima. The energy barrier to methyl group rotation taken from the Arrhenius plot of fig. 6 amounts to12 (±1) kJ/mol. With a pre-factor of 10^{-13}s one obtains 11 ps, compatible with the interpretation of type R.

The second time constant τ_{trans} in fig. 3 overlaps with experimental correlation times of protein hydration water (fig. 6), supporting a polar origin of type T. By fitting directly IN10 spectra of myoglobin-D_2O in the frequency domain, we derive a linewidth corresponding to τ_{trans} = 150 (±10) ps. This can be related to τ_{trans} = 145 ps, derived in the time domain. A mean square displacement parameter of δ^2 = 0,11 (± 0,015) $Å^2$ is deduced. The alternative fits show the variation of σ_m = 0,24 to 0,28, accounting for further methyl-like transitions.

In the dehydrated case, the second decay of type T is not observed. Most important, drying slows down methyl group reorientation by more than a factor of two. The fit to equ. 5 yields τ_{rot}(dry) = 18 (± 2) ps. We have checked this result by a spectral analysis of dry and hydrated myoglobin using IN6 and IN10. We obtain τ_{rot}(hydrated) ≅ 8,5 ps and 19 (± 2) ps for the dehydrated case, similar to the time domain results. Interestingly, the TR model fits disagree with the data at intermediate times ≅ 50 ps.

The fit to a stretched exponential with a stretching exponent of 0,7 and $\tau_{rot} \cong$ 25 ps can account for the full time range. Dehydration thus induces a dispersion of methyl side chains with increased barrier in a more compact rigid environment. However, the important long time plateau value of ≅0,8 is identical with the hydrated case, supporting the assignment to methyl groups.

Fig. 4 shows the intermediate scattering function of hydrated myoglobin covering an extended Q-range up to 4,8 $Å^{-1}$ at a slightly reduced time window. The fits to the TR model are conclusive, if we use the correlation times determined above as input (fig. 3). The MSD is adjusted, yielding, $\delta^2 = 0{,}12\ (\pm 0{,}02)\ Å^2$. The Brownian oscillator (equ. 6) would predict a much stronger Q-dependence. The quality of the fit, indicates, that the TR model reproduces the spatial distribution of displacements rather well.

c) Temperature dependent correlation times from elastic scattering functions

The elastic scattering profiles, measured with hydrated myoglobin are shown in fig. 5a, normalized at the lowest temperature of 10 K. To unravel the dynamic aspects of elastic scattering in a transparent manner, we have introduced the method of "elastic resolution spectroscopy"[3,22], where the resolution function is varied. In the simplest case of a δ-correlated resolution function[3], the normalized elastic intensity versus Q accurately reproduces the time correlation function at fixed resolution time:

$$S_{el}^{N}(Q) \cong \Phi_s(Q, \tau_{res}) \qquad (8)$$

Thus fitting elastic scans versus momentum exchange at fixed time τ_{res} by adjusting $\tau_{rot}(T)$ and $\tau_{trans}(T)$ in equs. 4 - 6, yields the requested dynamic information. At the next level of approximation the time functions in equ. 5 and 6 are replaced by a convolute with the exact resolution function of the spectrometer[3]. For the methyl group this analysis has been performed with dehydrated myoglobin, resulting in a prediction of the MSD(T) shown in fig. 1[8]. In the present context this procedure works rather well already at the level of equ. 8. Fits, taking into account the Gaussian resolution of IN 13, were also performed[3]. The most striking result is the absence of dynamical transitions: The fitted MSD parameter, $\delta^2 \cong 0{,}11\ (\pm 0{,}02)\ Å^2$ is almost independent of the temperature as demonstrated in fig. 1.

As an example, fig. 5 b) shows a decomposition of the elastic scan at 270 K into a Gaussian (Brownian oscillator) and the methyl incoherent structure factor based on the TR model. Equally important, the resulting correlation times $\tau_{rot}(T)$, displayed in fig. 6, compare well with those determined independently by a spectral analysis of dehydrated myoglobin and the methyl side chain of alanine dipeptide[3]. The methyl rotational barrier in the hydrated case is 11 (± 1) kJ/mol, the pre-exponential amounts to 1,6 $10^{13} s^{-1}$. Also, the translational correlation times, $\tau_{trans}(T)$, superimpose within experimental error with those derived for protein hydration water by neutron spectroscopy[3,23]. From the temperature dependence assuming an Arrhenius law one deduces a barrier of 17 (±1) kJ/mol with a pre-exponential rate factor of 7,5 10^{12} s^{-1}.

d) Multiple scattering

The analysis, presented above, assumes that each neutron on its passage through the sample is scattered only once. In real experiments at a transmission near 90% about 17 % of the neutrons are scattered twice[7,11,24]. Elastic-elastic second scattering events yield the dominant contribution due to the large dynamical structure factor of proteins at $\omega = 0$. The second scattering is approximately angle independent, which leads to an extra intensity at $Q = 0$. Since the elastic intensity decreases with rising temperature, multiple scattering also decreases. As a result, one always observes with elastic scans an extra intensity at $Q = 0$, which is decreasing with increasing temperature: $S_{el}(Q = 0, T)$. Therefore, except for the data in fig. 5 a, elastic scattering profiles are often normalized at each temperature and $Q = 0$. Several examples are given in ref.(1), which are incompatible with single scattering theory. This discrepancy has recently served as a main argument against conventional scattering theory[1]. In fig. 7 we display the elastic intensities derived from data presented partially in fig. 5a), which were extrapolated to $Q = 0$. It shows the effect of a temperature dependent elastic intensity at zero momentum exchange. Also shown are our calculations of the second order scattering for an infinite plane slap sample according to the method of Sears [11,25]. The calculated elastic-elastic second scattering curve reproduces the experiment rather well except at high temperatures, where quasi-elastic scattering dominates. Also shown are the reconstructed elastic intensities at zero Q of the green fluorescent protein [1]. Given the uncertainties of their extrapolation procedure and the

unknown transmission, multiple scattering seems to be a valid explanation for the GFP results.

IV. Discussion

We are now in a position to evaluate the difference between conventional scattering theory, termed by Frauenfeder the "spatial motion model" (SMM) and his "energy landscape model" of proteins (ELM)[1,2]: We compare the respective predictions of experimental results and their logic consistency. With ELM neutrons are treated as wave-packets of finite length exchanging momentum locally with protein protons, while the energy exchange occurs globally with the protein performing a random walk in energy space[1,2]. The idea of wave packets of finite length is not new and is also often used with regular scattering theory. To describe the scattering process and the role of the instrumental resolution in the time domain we wrote in 2003[22]: *If the primary spectrometer could select a sharp wavelength λ_0, an infinite plane neutron wave without time limitation would result. Instead, a narrow distribution of wavelengths of width $\Delta\lambda$ is selected, which leads to a finite coherence length. The finite length of the neutron wave packet, which moves with average velocity $v = h/(m_N\lambda_0)$ across the scattering centers limits the scattering time to* $t \leq \hbar/\Delta E_0 = m_N\lambda_0^3/(h\Delta\lambda)$. m_N *is the neutron mass and ΔE_0 denotes the width of the initial neutron energy distribution. Choosing λ_0 = 5,1 Å and $\Delta\lambda$ = 0,1 Å yields a resolution time window of 33 ps*…This explanation is "closely related" to statements in ref. 1 and 2, only we did not call it a "De Broglie" wave packet. With ELM, for further description of the scattering process one has to change somehow from the time domain to the energy domain. With SSM the complete scattering process can be discussed in the time domain in terms of the loss of temporal coherence of the phase factors: (1) the initial wavelength distribution and (2) the spatial motion of the sample protons: Incoherent scattering means that only the scattered neutron waves emanating from the same point source interferes in time modulated by the spatial displacement of the source. If the proton is not moving during the scattering time, the wave-packet emerges unchanged giving rise to a resolution-limited spectrum. The mathematical description of this process is expressed by the correlation function of the phase factor times the resolution function (equ. 1):

$$\Phi_s(Q,t) = \frac{1}{N}\sum_j < e^{i\vec{Q}\cdot\vec{r}_j(0)} \cdot e^{-\vec{Q}\cdot\vec{r}_j(t)} >_{powder} \cdot R(t,\lambda,\Delta\lambda) \quad (9)$$

N is the number of scattering centers j. In the time domain it is obvious, that the loss of coherence of the neutron wave in the sample is caused by spatial displacements of the scattering centers $\mathbf{r}_j(t)$ projected to the wave-vector **Q**, which acts as a spatial ruler: With small Q a large displacement is required to produce a significant loss of coherence. Vice versa, the detection of small displacements requires large wave-vectors. Neutron scattering is thus highly suitable to record molecular displacements, while it is much less suitable to characterize motions in energy space. It is thus not surprising that our well adapted spatial TR model can appropriately predict the outcome neutron scattering experiments with proteins. To demonstrate this fact we only Fourier transform the experimental spectra to the domain. As a result, fig. 3, two processes, well separated in time emerge, reflecting the loss of phase coherence caused by two types of molecular displacements. Their spatial characteristics can be probed by varying the Q-parameter as shown in fig. 4. Frauenfelder argues[1,2] that the distinction between elastic and quasi-elastic scattering is arbitrary or even unphysical. In the time domain it is easy to show, why this conclusion is incorrect[1]: The intermediate scattering function $\Phi_s(Q , t)$ can be split without loss of generality into a long time constant, $\Phi_s(Q, t \to \infty)$ = EISF(Q) and a time dependent part F(Q, t) with $F(Q, t \to \infty) = 0$:

$$\Phi_s(Q,t) = [1 - EISF(Q)] \cdot F(Q,t) + EISF(Q) \quad (10)$$

In the frequency domain, the first term of equ.(10) turns into the quasi-elastic spectrum, while the constant second term produces the elastic spectral component. This really important equation allows one to distinguish between solids or glasses and liquids[3,12,13]. Liquids do not show elastic scattering, thus EISF(Q) = 0. For this reason the elastic incoherent structure factor is also called the glass form factor: EISF(Q) > 0. The existence of a plateau between the two processes in the hydrated case and the long time plateau of the dry system in fig. 3 prove this distinction.

The intense elastic scattering versus temperature and momentum exchange is generally a good guide to detect the molecular processes before low intensity quasi-

elastic spectra are recorded. Fig. 1 and 2 indicate the presence of at two major processes with different temporal and spatial characteristics. The spatial TR model with only two major components reproduces the experimental data of hydrated myoglobin quantitatively, supporting the concept of an efficient molecular description of protein dynamics. This success is partially the result of two components, which are well separated in time and space. No evidence of further components due to nonpolar side chains and the main chain was found at this level of precision. The relaxation function of both components in the hydrated case is approximately exponential in spite of dynamical heterogeneity, although $\Phi_T(Q, t)$ of equ. 6 is intrinsically non-exponential. Most likely, at the high temperatures, significant motional narrowing by water reduces the width of the parameter distribution, as suggested by comparison with the more inhomogeneous dehydrated sample. A spread of the relaxation times within a factor of two could not be resolved. Data at higher precision are required, including low temperature experiments to check for a possible Q-dependence of the relaxation times in fig. 3 and 4.

It took more than 10 years until the important role of the methyl group in neutron scattering spectra of proteins was recognized. In 2001, the fast component of the intermediate scattering function of hydrated myoglobin at room temperature was assigned to methyl rotation[22]. Since the time domain data, comparable to those of fig. 3, were derived from elastic scattering spectra, the relevance of the resolution function in the dynamical transitions was established[22]. An extensive analysis of displacement distributions in proteins was published in 2005[8], where type R was definitely identified with methyl group rotation. Roh et al and Telling assigned the non-harmonic MSD onset at 100 K to methyl rotation[27,29]. Their onset temperature is rather low, compared to 150 K (140 K, IN10) of the type R transition[28]. Commercial preparations sometimes contain acetate and thus fast rotating acetyl groups, which cannot be easily removed as shown in ref. 3.

The first temperature and hydration dependent simulation of methyl groups in proteins was published in 2002 by Curtis et al.[26], suggesting, that in the dry case rotation is largely arrested. In the experiment, such transitions are nevertheless observed, although the transition rates are slowed down significantly. Furthermore, the dispersion of correlation times, deviating from exponential decay suggests an energy barrier distribution, which is not present in the hydrated case. Dehydration leads to a

more compact and rigid structure, which can differ between sites. A distribution of methyl energy barriers in lyophilized proteins with different structure was reported, applying a similar elastic analysis as in ref.(5)[29]. Methyl groups in proteins have also been observed by other methods like NMR[30]. But the type T water-coupled motions were first discovered by neutron scattering[5]. The relaxation times of protein hydration water, measured with different methods, and the slow component of myoglobin structural relaxation from neutron scattering experiments, are similar both in their absolute values and their temperature dependence, which is consistent with fig. 6[23]. Hydration water induces swelling, decreasing the local viscosity and, most important, reducing dynamical heterogeneity. The relevance of type T motions suggests a viscoelastic coupling of density fluctuations of hydration water and polar protein residues. This effect is better characterized as plasticization than by "slaving". Simulations suggest a mutual relaxation of the protein-solvent hydrogen bond network via solvent translational motion[26].

One of the strongest arguments in support of ELM is the temperature dependent elastic intensity at Q = 0, which is the main topic of ref. 1. The elastic decrease at zero Q with rising temperature is subtle and is usually removed by normalization at each temperature[1,3]. Fig. 5a) shows the original data of hydrated myoglobin without this correction. We understood this effect at about 1997 after performing extensive second scattering calculations[24]. The temperature dependence of the zero Q elastic intensity with increasing temperature reflects the decrease of multiple scattering, which is nearly Q-independent. The elastic intensity loss turns into quasi-elastic scattering. Fig. 7, which also includes some reconstructed results of GFP, shows that the calculations account quantitatively for this effect. Multiple scattering, although it contributes with 15 to 20 % to the scattering function (Supplement) is largely ignored in the literature. High precision experiments have to be corrected not only for absorption and self-shielding, but also for multiple scattering[8]. The observed temperature dependent elastic intensity at zero Q is thus not really supporting the validity of the energy landscape model. It is an unavoidable second order effect of single scattering theory.

V. Conclusions

The conventional space-time analysis of molecular motions in proteins yields strikingly consistent results, confirming the established scattering theory. For the first time a combined description of elastic and inelastic neutron scattering of proteins is possible, supporting the concept of homogeneous quasi-elastic scattering spectra. This does not exclude the existence of dynamical heterogeneity. The basic quantity of neutron scattering, $G(\mathbf{r},t)$ can be interpreted as a displacement distribution[8]. While in the hydrated case the protein fluctuations appear homogeneous apart from different dynamic processes, one observes a spread in relaxation times at reduced hydration within a single process. The spatial TR model thus can account for dynamic disorder without resorting to a landscape model. It requires just four parameters: two time constants, the translational displacements and the fractional cross section. This is what we call 'minimal complexity'. For comparison, molecular dynamic simulations of proteins involve force fields require numerous parameters as input. The landscape model does not produce quantitative predictions on the outcome of neutron scattering experiments and does not compete with the spatial approach.

Finally the novel features of the TR model are summarized:

1) The original model was defined by a sequential combination of two processes assuming identical sites, which can perform two kinds of motions. Only fits of the elastic scattering function were performed. The experiments with BR, where methyl groups were replaced by non-rotating side chains (fig. 1), prove the existence of at least two different sites, each performing one kind of motion. This leads to the parallel model of equ. (4). Since the R-sites have been assigned to methyl groups, one can fix the respective cross-sections.

2) The new parallel model unifies the description of elastic and quasi-elastic scattering functions. For this purpose we chose the time domain, because in this frame instrumental effects can be efficiently removed. The data obtained with several spectrometers with the same sample can be combined, expanding the time range to about 1000 ps. For the first time local translational motions of protein residues are approximated successfully by the Ornstein-Uhlenbeck process of an over-damped Brownian oscillator.

3) Combining a large time with an extended Q-range, which is technically demanding, was not done before. Only the backscattering instrument IN13 can provide the necessary Q^2 range of 25 $Å^{-2}$. Due to the low flux, such experiments require several day of beam time for a single temperature. For future experiments with new spectrometers, this suggests to focus on expanding the Q-range in addition to the time window.

4) A major new achievement is the removal of any "dynamical transition" from the temperature dependent displacements in fig. 1. With the TR model one derives temperature dependent correlation times from the elastic scattering function (Fig. 5a and 6) at the resolution time of the instrument. This procedure also yields the translational displacements, which show a linear temperature dependence (fig. 1), $\delta^2 = K_B T/(m\omega_0^2)$, characteristic of a harmonic potential. This does not include the vibrational displacements. Protein dynamics can now be discussed at high temperatures without involving any de-trapping from energy minima. In 2001 we had already shown by introducing 'elastic resolution spectroscopy' that the complete intermediate scattering of protein dynamics in the time domain could be derived from elastic scattering experiments by varying the instrumental resolution[22]. We call this the 'protein dynamical transition' observed at room temperature[3,22].

Our space-time analysis provides strong evidence for homogeneous quasi-elastic spectra of proteins. We obtain time constants of molecular processes, methyl rotation and relaxation of hydration water, which are well established in the literature by other methods. For inhomogeneous spectra[1,2], the TR model would fail. Our results thus provide no case against scattering theory[31]. The temperature dependent elastic intensity at zero momentum exchange, which has been used as a strong argument against conventional scattering theory[1], can be explained by multiple scattering. We also exclude the idea of a change in the protein force constants at the dynamical transition temperature, which was removed by the TR model[14].

Supplementary Material

See "supplementary material" for a more detailed description of the multiple scattering calculations presented in chapter III d).

Acknowledgements: I appreciate the assistance of the instrument scientists Winfried Petry and Bernhard Frick. My former collaborators Marcus Settles, Frank Post and Martin Diehl contributed with ideas and participation in some experiments, which is gratefully acknowledged. Franz Fujara suggested the application of IN13 to biomolecules. The late Edgar Lüscher is responsible for my engagement in neutron scattering, his activity promoted the decision to build the FRM2 in Munich.

References

1. Frauenfelder, H., Young, R. D., Fenimore, P.W. The role of momentum transfer during incoherent neutron scattering is explained by the energy landscape model. Proc. Natl. Acad. Sci. USA **114**, 5130-5135 (2017)

2. Frauenfelder, H., Fenimore, P.W., Young, R.D. A wave-mechanical model of incoherent quasi-elastic scattering in complex systems. PNAS USA **111**, 12764-12768 (2014).

3. Doster, W., Nakagawa, H., Appavou, M.S. Scaling analysis of bio-molecular dynamics derived from elastic neutron scattering experiments. J. Chem. Phys. **139,** 45105 -16 (2013)

4. Doster, A., Bachleitner, A., Dunau, R., Hiebl, M., Lüscher, E. Thermal properties of water in myoglobin crystals and solutions at subzero temperatures, Biophy. J. **50**, 213-219 (1986)

5. Doster, W., Cusack, S., Petry, W. Dynamical transition of myoglobin revealed by inelastic neutron scattering. Nature **337**, 754-756 (1989)

6. Doster, W., Cusack, S., Petry, W., Dynamical instability of liquid-like motions in a globular protein observed by inelastic neutron scattering, Phys. Rev. Lett. **95,** 1080-1083 (1990)

7. Cusack, S., Doster, W. Temperature dependence of the low frequency dynamics of myoglobin. Biophys. J. **58**, 243-251 (1990)

8. Doster, W., Settles, M., Protein-water displacement distributions. Biochim.Biophys. Act.**1749**,173-186 (2005)

9. Engler, N., Ostermann, A., Niimura, N, Parak, F. Hydrogen atoms in proteins: positions and dynamics, Proc. Natl. Acad. Sci. USA**. 100**,10243-10248 (2003)

10. Gaspar, A.M., Busch, S., Appavou, M., S., Häussler, W., Georgii, R., Su, Y., Doster, W. Using polarization analysis to separate coherent and incoherent scattering from protein samples, Biochim. Biophys. Act. **1804**, 76-82 (2010)

11. Bee, M., Quasielastic Neutron Scattering. p. 17, 107-147, 195 Adam Hilger, Bristol, Philadelphia (1988)

12. Squires, G. L. Introduction to the theory of thermal neutron scattering, Dover Books in Physics p. 101 (1978)

13. Lovesey, S., W., Dynamics of solids and liquids by neutron scattering, p. 1-10, Springer Verlag Heidelberg (1977)

14. Zaccai, J., How soft is a protein, a protein dynamics force constant measured by neutron scattering. Science **288**, 1604-1607 (2000)

15. Gabel, F., Bicout, D., Lehnert, U., Tehei, M., Weik, M., Zaccai, G. Protein dynamics studied by neutron scattering, Qu. Rev. Bioph. **35**, 327-367 (2002)

16. Doster, W., Concepts and misconceptions of the protein dynamical transition, Eur. Biophys. J. **37**, 591-602 (2008)

17. Gaspar, A., M., Appavou, M., S., Busch, S., Unruh, T., Doster, W. Dynamics of well folded and disordered proteins in solution: a time of flight neutron scattering study. Eur. Biophys. J. **37**, 573-582 (2008)

18. Lichtenegger, H., Doster, W., Kleinert, T., Birk, A., Sepiol, B., Vogl, G., Heme solvent coupling, a Mößbauer study of myoglobin in sucrose. Bioph. J. **76**, 414-422 (1999)

19. Settles, M., Doster, W., Anomalous diffusion of adsorbed water, a neutron scattering study of hydrated myoglobin, Faraday Disc. **103**, 269-280 (1996)

20. Doster, W. Brownian oscillator analysis of molecular motions in biomolecules in 'Neutron Scattering in Biology, techniques and applications' Eds. Fitter, J., Gutberlet, T., Katsaras, J., Springer, biological and medical physics, biomedical engineering , chapter 20, 461-482 (2006)

21. Risken, H. The Fokker Planck equation; methods of solution and applications, Springer , Berlin (1984)

22. Doster, W., Diehl, M., Petry, W., Ferrand, M., Elastic resolution spectroscopy: a method to study molecular motions in small biological samples. Physica B **301**, 65-68 (2001)

23. Doster, W., Busch, S., Gaspar, A., Appavou, M.S., Wuttke, J. . Scheer, J. Dynamical transition of protein hydration water, Phys. Rev. Lett. **104**, 098101-4 (2010)

24. Settles, M., Doster, W. Iterative calculations of the vibrational density of states from incoherent neutron scattering data with the account of double scattering. Biological Macromolecular Dynamics, 3-8, Adenine Press (1997)

25. Sears, V. Slow-neutron multiple scattering, Adv. Phys. **24**, 1-15 (1975)

26. Curtis, J.E, Tarek, M., Tobias, D.J. Methyl group dynamics as a probe of the protein dynamical transition, JACS **126**, 15929 (2004)

27. Roh, J.,H., Curtis, J., Assam, S., Novikov, V., Peral, I., Chowdhuri, Z., Gregory, R., Sokolov, A. Influence of hydration on the dynamics of lysozyme , Biophys. J. **91**, 2573-2588 (2006)

28. Schiro, G., Caronna, Ch., Natali, F., Cupane, A. Direct evidence of the amino acid side chain and backbone contributions to protein anharmonicity. J. Am. Chem. Soc. **132**, 1372-74 (2010)

29. Telling, M., T., Neylon, C., L., Kilcoyne, S., J., Arrighi, V.. Anharmonic behavior in the multisubunit protein apoferritin as revealed by quasi-elastic neutron scattering, J. Phys. Chem. B **112**, 10873-10878 (2008)

30. Lee, A., L., Wand, A., J., Microscopic origins of heat capacity and the glass transition in proteins. Nature **411**, 501-504 (2001)

31. Wuttke, J. No case against scattering theory, Proc. Natl. Acad. Sci. USA **114**, E8318/19 (2017)

32. Kneller, G. R. Inelastic neutron scattering from damped collective vibrations of macromolecules, Chem. Phys. **261**, 1-24 (2000)

33. Doster, W., Diehl, Gebhardt, R., M., Lechner, R. E., Pieper, J. TOF elastic resolution spectroscopy , time domain analysis of weakly scattering (biological) samples, Chem. Phys. **282**, 487-494 (2003)

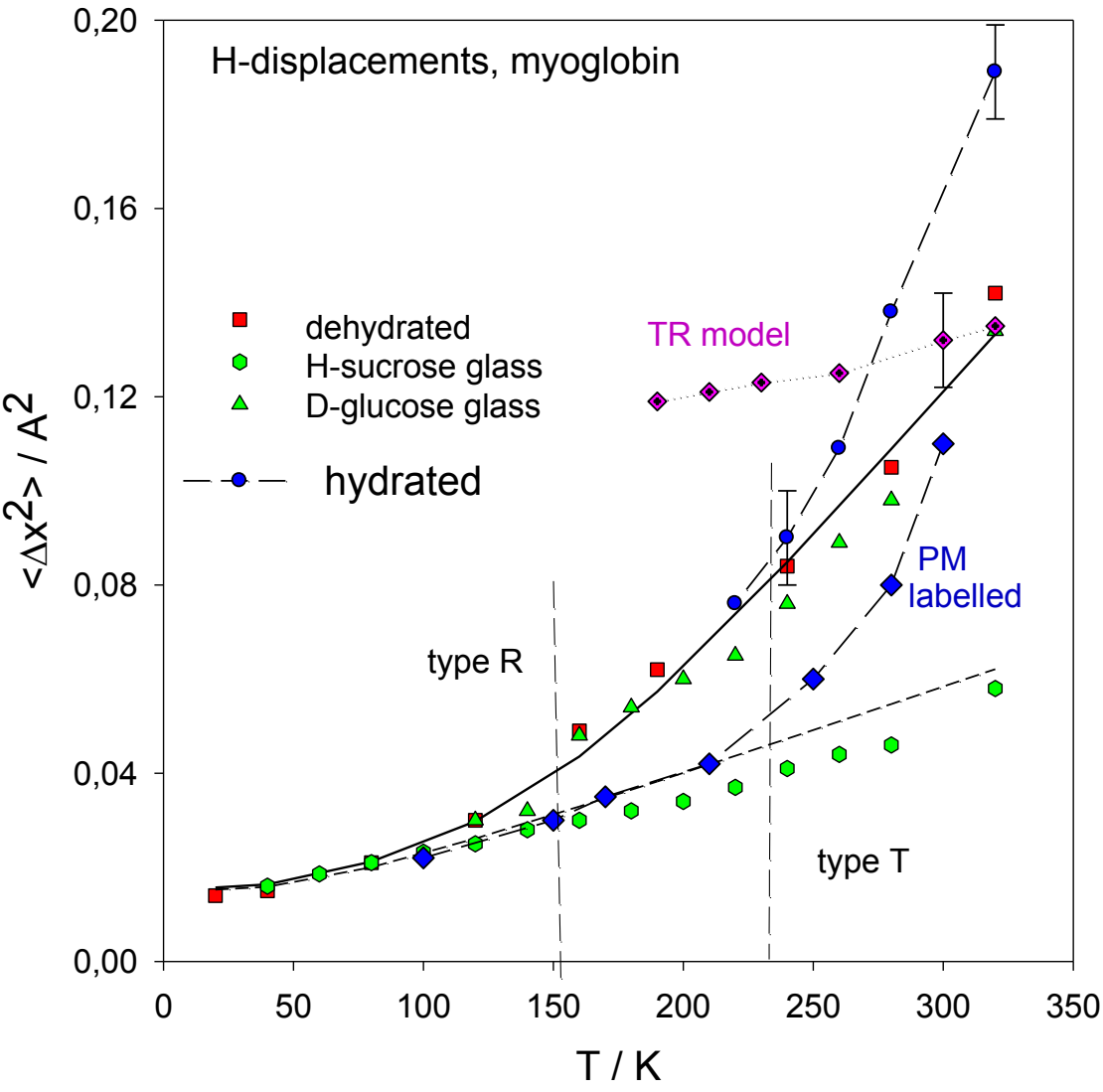

Fig. 1: MSD (IN13, τ_{res} = 140 ps) of myoglobin in various environments[1,5]: dehydrated (red squares), hydrated (blue circles), green triangles: per-deuterated glucose glass, green circles: D-H-sucrose glass[18,19], blue diamonds: H-labelled per-deuterated PM fragments[18], violet diamonds: δ^2 of TR model, thick line: predicted methyl group displacements[5], short dashed line: calculated vibrational displacement[25,26], vertical dashed lines indicate the onset temperatures at 150 K (R) and 240 K (T).

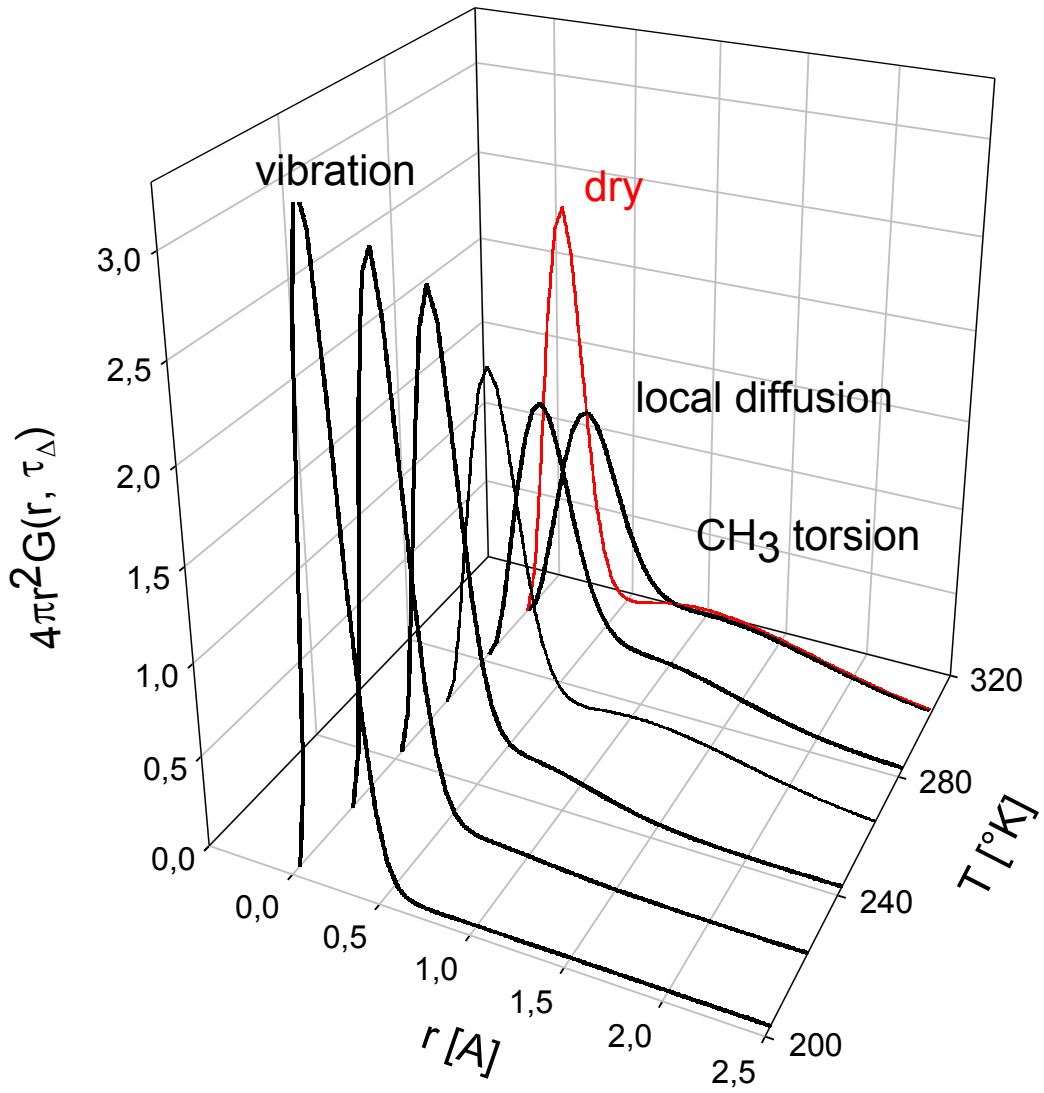

Fig. 2: Calculated displacement distribution functions of dry (red, 300 K) and hydrated myoglobin from a two-Gaussian fit of data in fig. 5a, versus displacement' r' and the temperature with three components, vibration, small scale translation (type T) and rotational transitions (type R)[2,5] at $\tau_\Delta \cong 140$ ps (IN13). In the dry state only vibrations and rotational transitions occur.

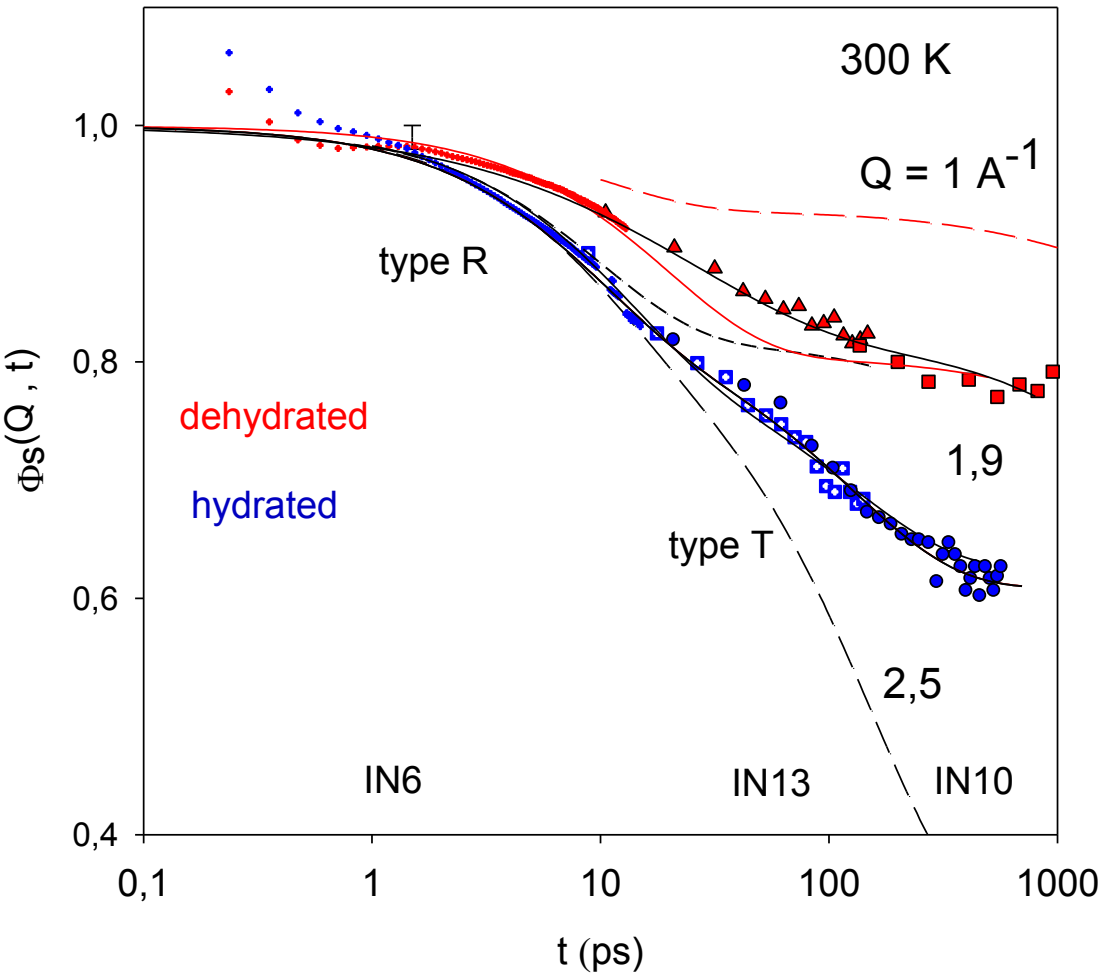

Fig. 3: Density correlation function of dry and hydrated myoglobin at 300 K and Q = 1,9(±0,1) Å^{-1}, combining the spectral information of three instruments as indicated, h = 0,35 g/g (blue), h < 0,05 g/g (red). Blue: full circles: IN10, open squares: IN13, dots: IN6. Red: squares IN10, triangles: IN13, dots: IN6. Full line: fits to equs.4 - 6 adjusting the time constants, τ_{rot} = 9 (±1) ps, τ_{trans}= 145 (±10) ps and δ^2= 0,11 (±0,015) Å^2. Short *dashed line, type R only. Red triangles and squares: dehydrated myoglobin, red line: type R fit, τ_{rot} = 18 (±2) ps, σ_m =0,25, black line: fit to a stretched exponential: τ_{rot} = 25 (±2)ps exponent: 0,7*

Figure 4

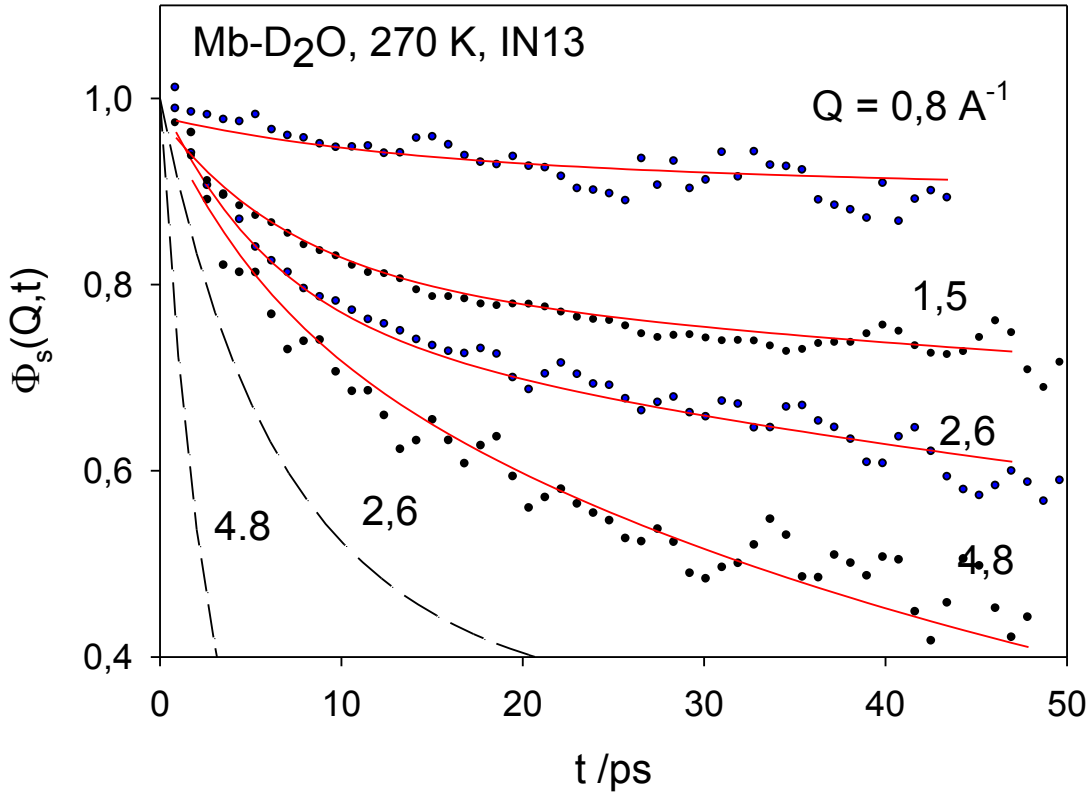

Fig. 4: Time domain density correlation function $\Phi_s(Q, t)$ of myoglobin-D_2O (0,35 g/g) (IN13) at various Q values. The red lines are the predictions of the TR model with $\delta^2 = 0{,}11(\pm 0{,}02)$ Å^2, $\tau_{rot} \cong 8$ (±2)ps and $\tau_{trans} \cong 120$ (±20) ps at 270 K. The dashed lines are the predictions of the Brownian oscillator of equ.6. The uncertainty of the Q-values is ± 0,1 Å^{-1}.

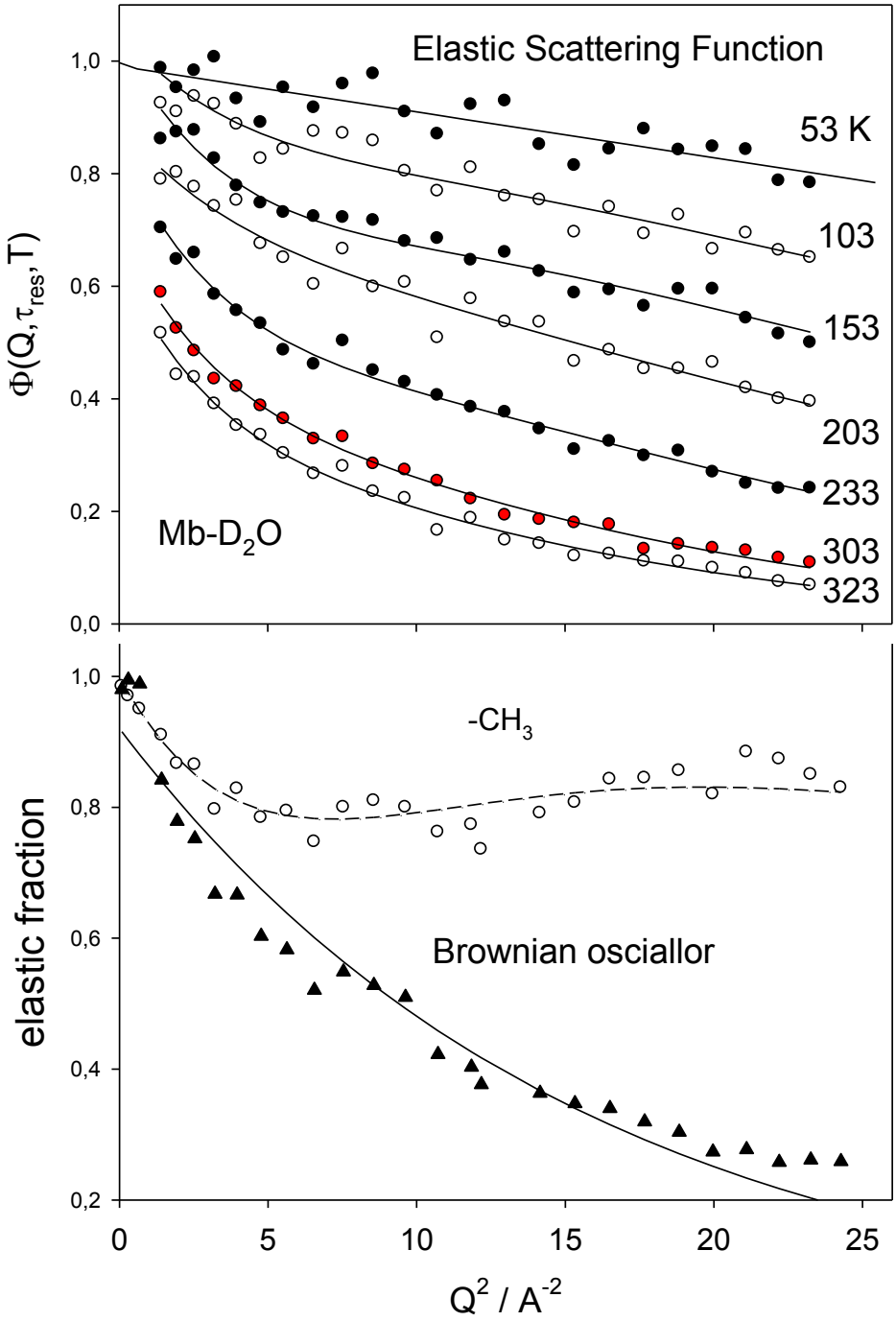

Fig.5 a): Elastic scattering profiles of hydrated myoglobin (0,35 g/g) normalized at 10 K, back-scattering spectrometer IN13 at τ_{res}= 140 ps and TR-fits by adjusting $\tau_{rot}(T)$ and $\tau_{trans}(T)$ with δ^2= 0,1 Å^2 kept fixed (full line).

b) *Decomposition of the elastic scattering function of hydrated myoglobin at* 270 K *according to the TR-model, the full lines are predictions of equs.5 and 6.*

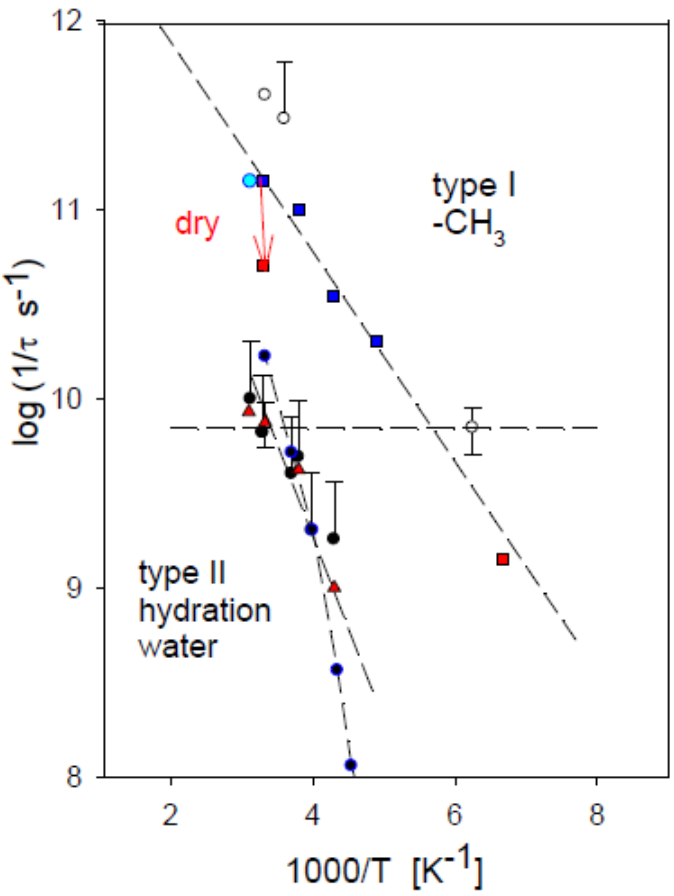

Fig. 6: Arrhenius plot of the fitted correlation times, blue squares: τ_{rot} from TR model fit, open circles: alanine dipeptide[1], light blue circle: IN10 spectral analysis of hydrated myoglobin, red squares: fit of IN6 spectrum of dry myoglobin, red arrow: transition from hydrated to dry, red triangle: τ_{trans} from TR fit, dark blue and black circles: τ_{hyd} , hydration water from ref. 1 and 8, horizontal dashed line: τ_{res} = 140 ps (Instrument IN13, the other dashed lines along red triangles, blue squares and blue circles are Arrhenius fits of τ_{rot}, τ_{trans} and τ_{hyd} respectively.

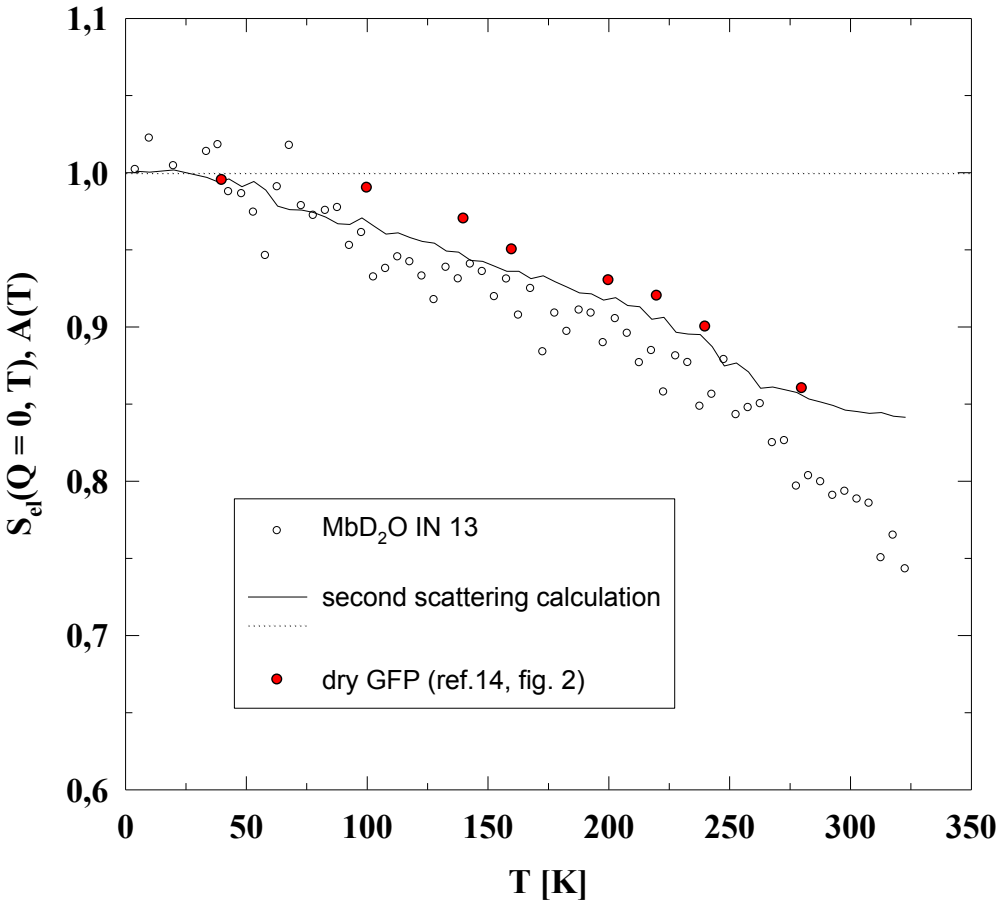

Fig. 7: Multiple scattering derived from extrapolation of the elastic intensity (fig. 5a) to Q = 0 of hydrated myoglobin (open circles) and of dehydrated GFP(full red circles) [14], full line: second scattering calculation assuming elastic-elastic scattering from an infinite flat cell according to Sears[39].